Catalysis Letters Vol. 105, Nos. 1–2, November 2005 (© 2005)
DOI: 10.1007/s10562-005-8012-2

Activation of $VOHPO_4 \cdot 0.5H_2O$ in propane/air mixture: effect on structural, morphological, oxidant's behaviour and catalytic property of $(VO)_2P_2O_7$ catalysts for propane oxidation

Y. H. Taufiq-Yap*, C. S. Saw, and R. Irmawati

Department of Chemistry, Universiti Putra Malaysia, 43400 UPM Serdang, Selangor Darul Ehsan, Malaysia

Received 15 June 2005; accepted 2 August 2005

$VOHPO_4 \cdot 0.5H_2O$ synthesized by $VOPO_4 \cdot 2H_2O$ and isobutanol was activated in a flow of propane/air mixture (1% propane in air) at 673 K for 36, 75 and 132 h. Three vanadyl pyrophosphate catalysts obtained were denoted as VPD36P, VPD75P and VPD132P. The crystallinity of all propane/air pretreated catalysts as shown in XRD increased with the duration of calcination. SEM micrographs showed the formation of more isolated platelets and more prominent rosebud-shape agglomerate as the pretreatment was longer. Four reduction peaks maxima at 752, 920, 1026 and 1140 were observed in the rate of hydrogen consumption for VPD36P. As the calcination duration increased to 75 h, the H_2 reduction peaks were shifted to lower temperatures at 750, 882, 1004 and 1140 K. When the calcination duration was further increased to 132 h, only three reduction peaks were observed at 752, 952 and 1142 K. Despite the progressively shifted of the major reduction peak maximum as the duration of calcination increased from 36 to 132 h, the lattice oxygen from VPD36P was found to be the most reactive. The catalytic performance for propane oxidation to acrylic acid (AA) showed that VPD36P gave the highest activity (9.6%) with 83.0% of selectivity to AA.

KEY WORDS: vanadyl pyrophosphate; propane oxidation; acrylic acid.

1. Introduction

The global abundance of low alkane and the huge economic incentives of converting them to various highly desirable petrochemicals of feedstocks for more valuable chemicals have stimulated an enormous amount of interests to explore selective oxidation processes to accomplish such conversions [1,2]. These processes include oxidative dehydrogenation, ammoxidation and selective oxidation [3]. The best-known selective oxidation of lower alkanes is the selective oxidation of *n*-butane to maleic anhydride (MA) over vanadium phosphorus oxide catalysts (VPO) [4]. It is, so far, the only successful industrial process utilizing alkanes [5]. The excellent performance of VPO catalyst in *n*-butane selective oxidation has stimulated great interests in propane selective oxidation to acrolein and acrylic acid (AA). Ai [6] reported that VPO catalyst is one of the catalysts giving the best performances among those proposed for propane oxidation although AA selectivity and the yields are still low. The yield of AA reached 7.5 mol% at the propane conversion of 46%; the selectivity is about 15 mol% [3]. Nowadays, AA is produced through a double step process starting from propylene [3]. A single step process using propane as feedstock would significantly reduce both cost and pollution [7].

$(VO)_2P_2O_7$ was found to be the major crystal phase in VPO catalysts active in *n*-butane oxidation [4] and propane oxidation [8]. In this paper, the effect of varying the duration of the propane/air pretreatment at 673 K upon the structural, morphological and catalytic performances of the $(VO)_2P_2O_7$ catalysts produced for propane oxidation to AA are investigated.

* To whom correspondence should be addressed.
E-mail: yap@fsas.upm.edu.my

2. Experimental

2.1. Catalysts preparation

The catalysts were prepared via dihydrate method [9]. Vanadium pentoxide, V_2O_5 (15.0 g from Fluka), was suspended by rapid stirring into a mixture of *o*-H_3PO_4 (60 mL, 85% from Merck (71.75 cm^3) and water (360 cm^3). The vanadium oxide–acid mixture was stirred and refluxed for 24 h at 393 K. The mixture was then cooled to room temperature. The yellow solid was recovered by filtration, washed sparingly with water and oven dried at 383 K for 24 h. $VOPO_4 \cdot 2H_2O$ was then refluxed with isobutanol (1 g 20 mL^{-1}) for 21 h and the solid product was recovered by filtration and oven dried at 383 K for 21 h to obtain the precursor, $VOHPO_4 \cdot 0.5H_2O$, denoted VPDpre. The resulting precursor, which was shown to be a well-crystallized $VOHPO_4 \cdot 0.5H_2O$ by X-ray diffraction (XRD) analysis, was then calcined under a flow of propane/air mixture (1% propane in air) at 673 K for 36, 75 and 132 h. The resulting catalysts were denoted VPD36P, VPD75P and VPD132P, respectively.

2.2. Catalysts characterization

The total surface area of the catalysts was measured by BET (Brunauer–Emmer–Teller) method using N_2 adsorption at 77 K. This was done by using Thermo-Finnigan Sorptomatic 1990 nitrogen adsoprtion/desorption analyzer.

XRD analyses were carried out using a Shimadzu diffractometer model XRD 6000 employing CuK_α radiation to generate diffraction patterns from powder crystalline samples at ambient temperature.

The bulk chemical composition was determined by using a sequential scanning inductively coupled plasma-atomic emission spectrometer (ICP-AES) Perkin Elmer Emission Spectrometer model Plasma 1000.

SEM was done using a Jeol JSM-6400 electron microscope. The samples were coated with gold using a sputter coater.

TPD (temperature-programmed desorption) and TPR (temperature-programmed reduction) analyses were done using a ThermoFinigan TPDRO 1110 apparatus utilizing a thermal conductivity detector (TCD).

2.3. Catalytic oxidation of propane

The oxidation of propane to AA was carried out at 673 K in a fixed bed multitubular reactor with a standard volume of catalyst (0.5 mL). A feedstock containing propane, oxygen, nitrogen and steam (ratio = 1/2/18/9) with GHSV = 1200 h^{-1} was introduced to the reactor. The products were then fed via heated lines to an on-line gas chromatography for analysis.

3. Results and discussion

3.1. BET surface area measurement, chemical analysis & redox titration

The total surface area of VPD36P, VPD75P and VPD132P are 13.4, 17.2 and 18.1 $m^2\ g^{-1}$, respectively. The prolonged duration of calcination from 36 to 75 and 132 h in propane/air environment increased the surface area. Furthermore, these surface areas are also higher than those reported by Landi *et al.* [9].

Chemical analysis using ICP indicated that the respective bulk P/V ratio for VPD36P, VPD75P and VPD132P are similar i.e. 1.09. Lin [3] reported that the VPO catalysts with P/V ratio at 1.15 were found to have high selectivity of AA over a wide range of propane conversion rate. Trifiró [10] also reported that P/V ratio is one of the key factors in catalyst preparation to avoid the oxidation of $(VO)_2P_2O_7$ and/or of the intermediate amorphous phase to a V^V phosphate.

The average oxidation number and percentage of V^{III}, V^{IV} and V^V oxidation state are shown in table 1. The result shows that increasing the duration of calcination did not affect the average oxidation number of vanadium. An increasing of the V^{IV} and a decrease of the V^V as the calcination time prolonged stabilised the average oxidation number of vanadium. An interesting point to be highlighted here is that the observation of V^{III} species in all these catalysts. This species was not found in the VPO catalysts calcined in *n*-butane/air mixture environment [11]. The role of V^{III} was also not well understood in the *n*-butane oxidation. Cavani *et al.* [12] suggested that the presence of V^{III} species may enhance the specific activity of in *n*-butane oxidation, while the selectivity to MA at low *n*-butane conversion (30%) remains substantially unaffected. However, Wang *et al.* [13] reported that accumulation of V^{III} species represents one mode of catalyst deactivation.

3.2. X-ray diffraction

The XRD pattern of the precursor, VPDpre (figure 1) was identical and in good agreement with those reported for $VOHPO_4 \cdot 0.5H_2O$, with peaks at $2\theta = 15.5°$, 19.6°, 24.14°, 27.0° and 30.4° [14,15]. The peaks at $2\theta = 15.5°$ and 30.4° were corresponds to (001) and (130) reflections, respectively, and the (130) reflection was the dominant feature in the precursor. This is the characteristic for the precursor prepared by using dihydrate method [9].

The XRD patterns for VPD36P, VPD75P and VPD132P catalysts which were prepared by calcination of the same precursor at 673 K under the flow of propane/air mixture (1.0% propane in air) for different duration on stream, i.e., 36, 75 and 132 h, are shown in figure 1. These catalysts showed crystallized $(VO)_2P_2O_7$ formed with the main peaks observed at $2\theta = 22.9°$, 28.4° and 29.9°, which corresponds to (020), (204) and (221) planes, respectively. The XRD pattern for VPD36P consists of a poorly crystallite phase of vanadyl pyrophosphate. However, as the duration increased to 75 and 132 h of calcination, the pyrophosphate peaks were raising and being more intense.

Table 1
Average oxidation numbers and percentages of V^{III}, V^{IV} and V^V oxidation states present in VPD36P, VPD75P and VPD132P

Catalysts	Average oxidation number	V^{IV} (%)	V^V (%)	V^{III} (%)
VPD36P	4.09	69.1	13.8	17.1
VPD75P	4.09	72.4	11.9	15.7
VPD132P	4.08	76.0	9.8	14.2

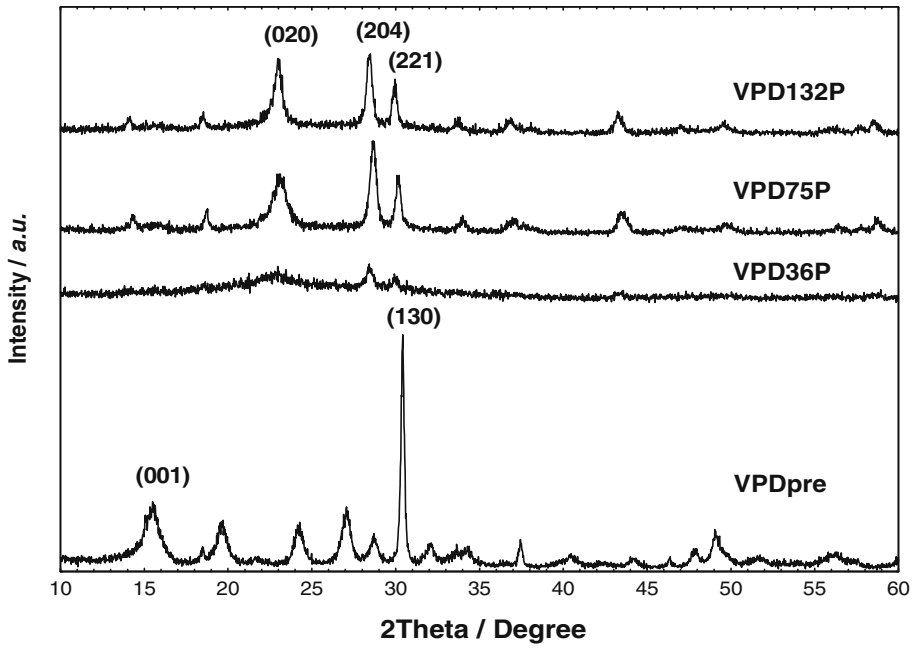

Figure 1. XRD patterns of VPDpre, VPD36P, VPD75P and VPD132P.

The FWHM values of the XRD reflection can be used to determine the extent of structural disorder [16]. Table 2 shows the line width of the (020) and (204) plane reflections and the particles thickness for (020) and (204) phase of the catalysts. The parameter used to determine the crystal size of the catalysts is the half width of the (020) reflection. The line width increases with the decreasing of the crystallites size. The decrease of the FWHMs of the (020) reflection indicates that the particles thickness in the (100) direction increases. However, the half width of the (204) reflection changes slightly, reflecting a constant order of the *bc* plane, as well.

The particles thickness is given by the Debye–Scherrer equation [17]:

$$t = \frac{0.9\lambda}{\beta_{hkl}\cos\theta_{hkl}},$$

where t is the particle thickness for (hkl) phase, λ is the X-ray wavelength of radiation for CuK_α, β_{hkl} is the full width at half maximum (FWHM) at (hkl) peak in radian and θ_{hkl} is the diffraction angle for (hkl) phase. The particle thickness for VPD36P at (020) and (204) were as calculated from the above formula are 90.21 and 164.05 Å, respectively, while for VPD75P these values are 92.22 and 179.77 Å, respectively. VPD132P gave higher value for particle thickness of (020) plane with 120.00 Å while a lower value for (204) plane i.e. 145.43 Å.

Table 2
XRD data for VPD36P, VPD75P and VPD132P catalysts

Catalysts	[a]FWHM $_{(020)}$/°	[b]FWHM$_{(204)}$/°	[c]$t_{(020)}$/Å	[c]$t_{(204)}$/Å
VPD36P	0.9	0.5	90.21	164.05
VPD75P	0.88	0.456	92.22	179.97
VPD132P	0.676	0.564	120	145.43

[a]Full widths at half maximum of (020) reflection.
[b]Full widths at half maximum of (204) reflection.
[c]Particle thickness calculated using Debye–Schrer equation.

3.3. Scanning electron microscopy

Figure 2 shows the morphological change of the catalysts followed by SEM after various duration of pretreatment in propane/air. The principal structures of the catalysts are the same: they show spheres resembling a rosebud with variable sizes but in a uniform shape [18]. However, the amounts of this characteristic rosebud-type agglomerate are affected by the duration of calcination. VPD132P appeared to have clearer and the most prominent rosebud-shape agglomerates and also have more isolated platelets compared to the less calcined catalysts, VPD36P and VPD75P. These are consistence with the observation whereby the amount of these rosebud-type agglomerates slightly increased as calcination time increased.

3.4. O_2 temperature-programmed desorption

The oxygen desorption spectra shown in figure 3 were obtained by pretreating the catalysts by heating them to 673 K in an oxygen flow (101 kPa, 25 cm^3 min^{-1}) and holding them under that flow at 673 K for 1 h before cooling them to ambient temperature. The flow was then switched to helium (1 bar, 25 cm^3 min^{-1}) and the temperature was raised (10 K min^{-1}) to 1173 K following the conductivity of the oxygen by a thermal conductor detector.

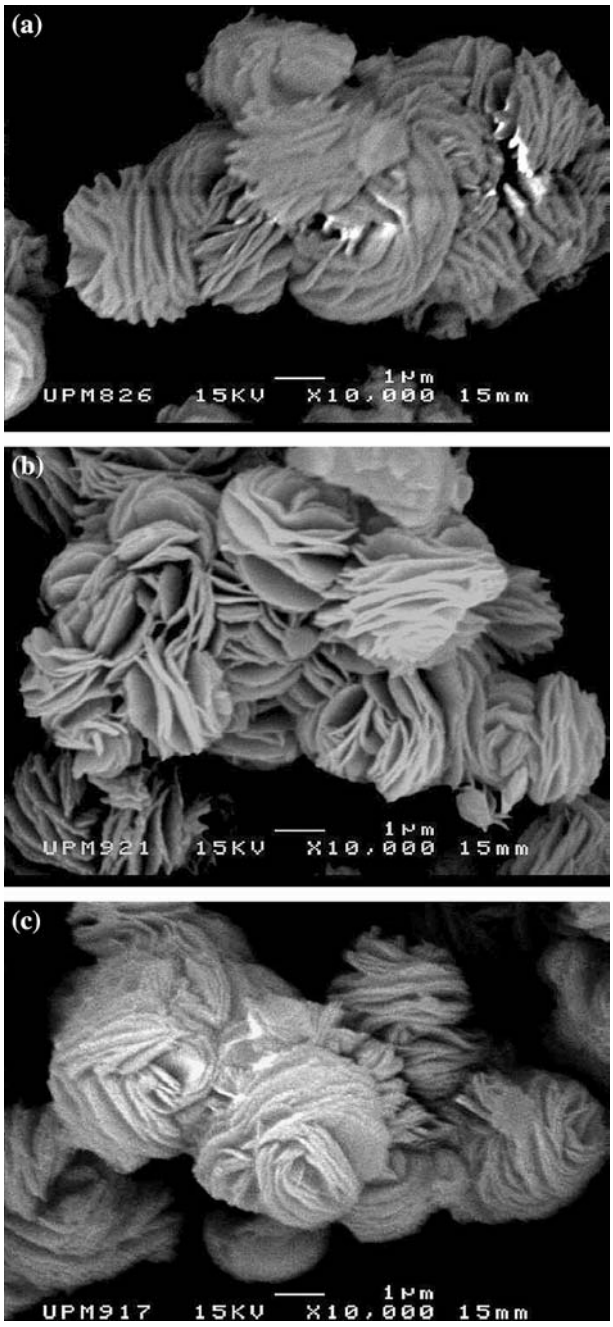

Figure 2. SEM micrographs of (a) VPD36P, (b) VPD75P and (c) VPD132P catalysts.

The onset of O_2 evolution for VPD36P occurs at ~800 K with a peak maximum observed at 969 K. The total amount of oxygen desorbed was 2.52×10^{20} atom g^{-1} (table 3). However, as calcination time increased to 75 and 132 h, the total amount of oxygen desorbed were found reduced to 1.99×10^{20} and 2.21×10^{20} atom g^{-1}, respectively. This phenomena where longer duration of calcination in the propane/air mixture produced catalysts which desorbed less oxygen is in good agreement with the result for the *n*-butane/air pretreatment reported earlier [19,20]. However, the reduction is only ~12–20% compared to a decreased of 50% of total amount of oxygen desorbed being observed from catalysts calcined in *n*-butane/air mixture. This may suggest that the development of extended defect is lower in propane/air environment which due to propane is less active than *n*-butane.

3.5. Temperature-programmed reduction

Figure 4 show the TPR profiles in a H_2/Ar stream (5% H_2 in Argon, 1 bar, 25 cm^3 min^{-1}) for VPD36P, VPD75P and VPD132P. The TPR analysis were carried out by pretreating the fresh sample of catalyst by heating them to 473 K in a nitrogen flow (1 bar, 20 cm^3 min^{-1}), holding them under the stream at 473 K for 30 min, before cooling them to ambient. Then the temperature was raised from ambient to 1273 K at 10 K min^{-1} in a H_2/Ar stream (5% H_2 in Argon, 1 bar, 25 cm^3 min^{-1}). The peak maxima temperature, the amounts of oxygen removed from each peak and the derived reduction activation energies are shown in table 4.

The reduction profiles of vanadyl pyrophosphate catalyst prepared via dihydrate method and calcined in *n*-butane/air mixture environment as reported earlier [11] was characterized by three reduction peaks maxima, α, β and γ occurred at 863, 1011 and 1143 K. However, the introduction of propane/air pre-treatment in this study induced the development of an additional new peak, α_1 which formed at a remarkably low temperature at ~750 K. Three other reduction peaks maxima for VPD36P occurred at 920, 1026 and 1140 K whereas VPD75P gave two reduction peaks, α and β peaks which shifted towards lower temperatures at 882 and 1004 K. The γ peak remained at 1140 K. However, an increase of calcination duration to 132 h resulted with the disappearance of α peak. Interestingly, the major peak i.e. β peak was significantly shifted to α peak region at 952 K. A close examination of the spectra at low temperature range (500–850 K) shows that VPD36P gave the highest

Table 3
Total number of oxygen desorbed and desorption activation energies obtained by TPD for VPD36P, VPD75P and VPD132P

Catalysts	T_{onset}/K	T_{max}/K	Desorption activation energy, E_d/kJ mol^{-1}	O_2 atom desorbed from the catalysts/$\times 10^{-4}$ mol g^{-1}	O_2 atom desorbed from the catalysts/$\times 10^{20}$ atom g^{-1}
VPD36P	800	969	267.5	4.18	2.52
VPD75P	859	971	268.1	3.32	1.99
VPD132P	870	979	270.3	3.68	2.21
VPD75B [19]	840	1011	276.4	5.12	3.08

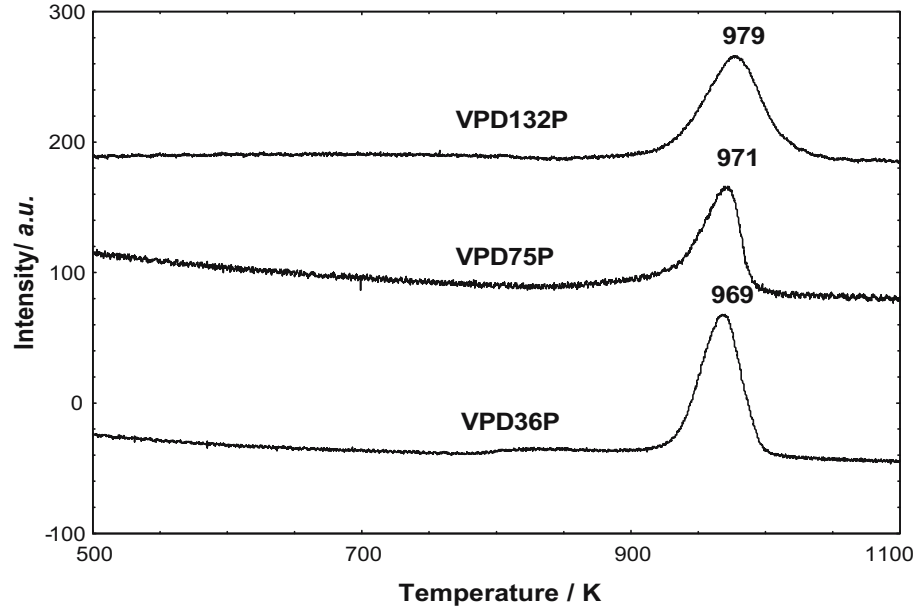

Figure 3. Temperature-programmed desorption of O_2 from VPD36P, VPD75P and VPD132P catalysts.

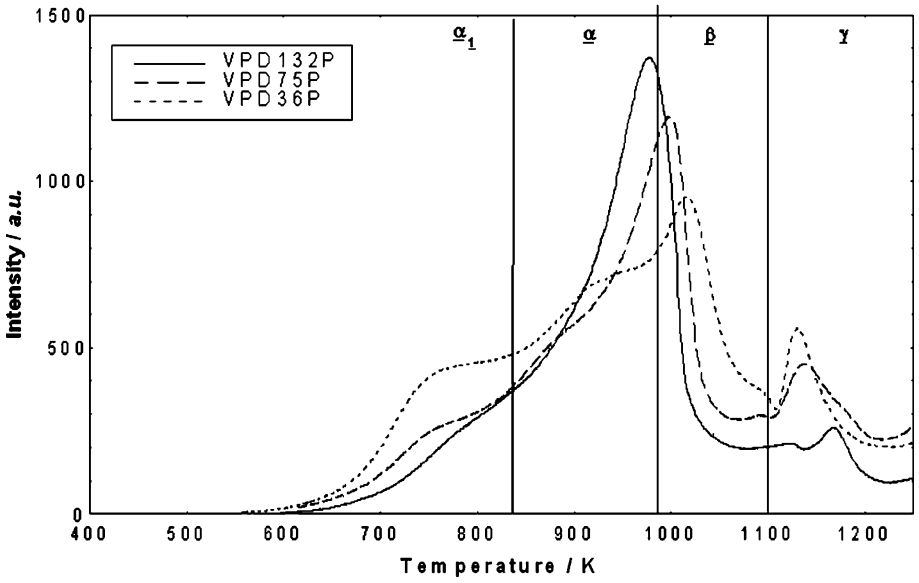

Figure 4. Temperature-programmed reduction in H_2 for VPD36P, VPD75P and VPD132P catalysts.

reducibility with higher rate of reduction. Furthermore, VPD36P also appeared to remove the highest total amount of oxygen atoms at this region. Our previous result shows that significant increased in the *n*-butane conversion was obtained when the major reduction peak (β) was shifted from 1011 to 906 K for bismuth-promoted VPO catalysts [11,21].

3.6. Catalytic oxidation of propane

The catalytic performance of VPD36P, VPD75P and VPD132P are shown in table 5. The increasing of duration of calcination slightly decreased the propane conversion. Thus, 9.6% of propane conversion was achieved by VPD36P catalyst, while only 8.7 and 7.9% of propane conversion rate were obtained by VPD75P and VPD132P, respectively. Reduction behaviour as shown in figure 4 and discussed earlier related to the catalytic performance of VPD36P which gave the highest activity. The result suggested that the activity of the catalyst dependences on the mobility and reactivity of the lattice oxygen. The decreasing of propane conversion may also suggest a correlation between the amounts of V^V species in the catalysts with the catalytic performance of the catalyst, as shown in figure 5. The amount of V^V species for VPD36P was 13.8% and the value reduced to 11.9 and 9.8% for VPD75P and VPD132P, respectively. It has been reported that V^V species play a specific role in the hydrogen abstraction from *n*-butane

Table 4
Amount of oxygen removed and reduction activation energies obtained by TPR of H_2 with VPD36P, VPD75P and VPD132P

Peaks	T_{max}/K	Reduction activation energy, E_r/kJ mol^{-1}	O_2 atom removed from the catalysts/$\times 10^{-3}$ mol g^{-1}	O_2 atom removed from the catalysts/$\times 10^{21}$ atom g^{-1}
VPD36P				
α_1	752	125.77	0.687	0.42
α	920	153.86	0.992	0.60
β	1026	171.59	1.145	0.69
γ	1140	190.66	0.198	0.12
Total O_2 atom removed			3.022	1.83
VPD75P				
α_1	750	125.4	0.338	0.20
α	882	147.5	0.565	0.34
β	1143	167.9	1.455	0.88
γ	1140	190.7	0.162	0.10
Total O_2 atom removed			2.520	1.52
VPD132P				
α	752	125.8	0.375	0.23
1				
β	952	159.2	2.02	1.22
γ	1142	191.0	0.031	0.02
Total O_2 atom removed			2.426	1.47
VPD75B [19]				
α	863	144.3	1.35	0.81
β	1011	169.1	2.10	1.26
γ	1143	191.1	0.76	0.45
Total O_2 atom removed			4.21	2.52

Table 5
The catalytic performance of VPD36P, VPD75P and VPD132P in propane

Catalysts	Propane conversion (%)	AA yield (%)	AA selectivity (%)	Acetic acid selectivity (%)	CO selectivity (%)	CO_2 selectivity (%)
VPD36P	9.6	8.0	83.0	5.5	0.0	2.8
VPD75P	8.7	7.6	87.6	3.2	0.0	1.6
VPD132P	7.9	6.4	81.5	3.6	0.0	2.2

[3]. Han *et al.* [8] also reported that the presence of a minor $VOPO_4$ (V^V) phase in $(VO)_2P_2O_7$ was shown to be effective for propane oxidation. A similar relation was also observed for V^{III} species (figure 5). VPD36P which found to have the higher amount of V^{III} shown to be the most active agree with the suggestion by Cavani *et al.* [12] on the role of V^{III} phase.

The AA selectivity for the catalysts does not uniformly increases with the duration of calcination, showing 83.0% AA selectivity for VPD36P and a slightly higher for VPD75P with 87.6% and a further decrease to 81.5% for VPD132P. However, a close examination and comparison of FWHM values with the AA selectivity of catalysts, as shown in table 6 and figure 6 concluded that AA selectivity reversely proportional with the FWHM value of (204) plane for vanadyl pyrophosphate. Although, the role of the crystalline structure of VPO catalysts in propane oxidation to AA is yet to be confirmed, the response of our catalysts (especially the selectivity of AA) seems to suggest that the (204) plane also play an important role in the AA formation.

Morphological structure of the VPO catalysts also affected the catalytic performance of the catalysts in propane oxidation to AA. Our catalysts which in rosette shape clusters show higher AA selectivity compared to those which mainly constituted of small lamellae (~32%) [10]. A higher AA selectivity achieved by our catalysts also can be explained by a higher total surface area obtained which mostly associated with the high development of the $(VO)_2P_2O_7$. Furthermore, our catalysts here were prepared via $VOPO_4{\cdot}2H_2O$ i.e. dihydrate method which also reported to have higher surface area and selectivity in *n*-butane oxidation [9].

These catalysts were also shown to inhibit further oxidation of the intermediate and/or the desired product. No CO could be detected by online GC and the selectivity for CO_2 was only about 2%. It is interesting to look at the performances of the catalysts in view of these one-step productions of AA from propane by using our novel modified vanadium phosphate catalyst. The highest AA selectivity obtained in this study (87.6%) compared favourably to the value of 20–60%

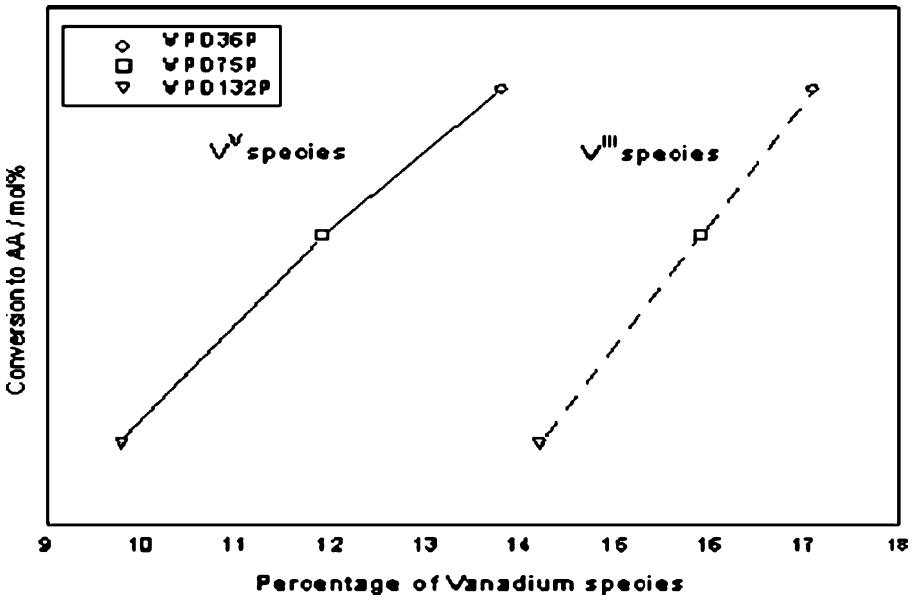

Figure 5. Changes of conversion of propane as a function of percentage of V^V and V^{III} species in the catalysts (VPD36P, VPD75P and VPD132P).

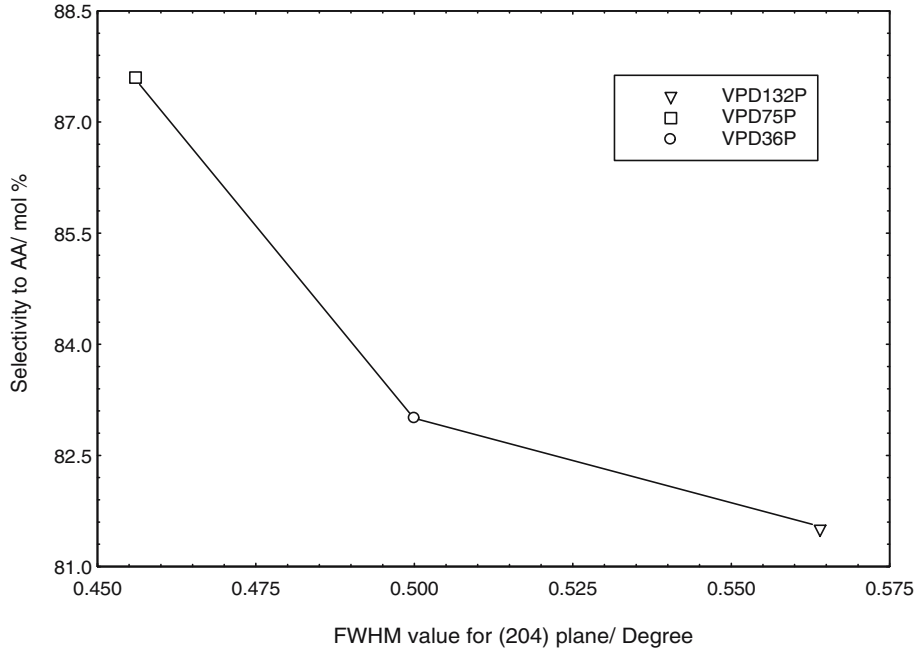

Figure 6. Changes of AA selectivity as a function of FWHM values for (204) plane.

(using Mo-based catalysts) given in the open literatures [22–24] or other reports on VPO catalysts i.e. Te/VPO (22%) [6], Ce/VPO (68%) [25] and $VPZR_{0.5}O_x$ (81%) [8]. Taking the reduction pattern obtained from TPR study as a guideline for further development of a better catalyst, it appears that the removal of a kinetically different type of oxygen atoms from the lattice will determine the reactivity of the catalysts.

Table 6
The correlation of FWHM value of (204) plane with selectivity to AA

Catalysts	FWHM $_{(204)}$/°	AA selectivity (%)
VPD36P	0.5	83.0
VPD75P	0.456	87.6
VPD132P	0.564	81.5

Acknowledgement

Financial assistance from Malaysian Ministry of Science, Technology and Innovation is gratefully acknowledged.

References

[1] R.K. Grasselli, Catal. Today 49 (1999) 141.
[2] M. Baerns and O. Buyevskaya, Catal. Today 45 (1998) 13.
[3] M.M. Lin, Appl. Catal. A: Gen. 207 (2001) 1.
[4] F. Cavani and F. Triffiro, Catal. Today 11 (1994) 246.
[5] G. Centi, Catal. Today 16 (1993) 1.
[6] M. Ai, Catal. Today 101 (1986) 389.
[7] G. Landi, L. Lisi and J.C. Volta, Chem. Commun. (2003) 492.
[8] Y. Han, H. Wang, H. Cheng, J. Deng, J.Chem. Soc., Chem. Commun. (1992) 803.
[9] G. Landi, L. Lisi and J.C. Volta, J. Mol. Catal. A:Chem. 222 (2004) 175.
[10] F. Trifirò, Catal. Today (1998) 21.
[11] Y.H. Taufiq-Yap, K.P. Tan, K.C. Waugh, M.Z. Hussein I. Ramli and M.B. Abdul Rahman, Catal. Lett. 89 (2003) 87.
[12] F. Cavani, S. Ligi, T. Monti, F. Pierelli, F. Trifirò, S. Albonetti and C. Mazzoni, Catal. Today 61 (2000) 203.
[13] D. Wang, H.H. Kung and M.A. Barteau, Appl. Catal. A:Gen. 201 (2000) 203.
[14] S. Albonetti, F. Cavani, F. Triffiro, P. Venturoli, G. Calestani, M.L. Garades and J.L.G. Fierro, J. Catal. 160 (1996) 52.
[15] J.M. Hermann, P. Vernoux, K. Bere and M. Abon, J. Catal. 167 (1997) 106.
[16] L.M. Cornaglia, C.R. Carrara, J.O. Petunchi and E.A. Lambardo, Appl. Catal. A: Gen. 183 (1999) 177.
[17] P.H. Klug and E. Alexander, *X-ray Diffraction Procedures for Polycrystalline and Amorphous Materials*, 2nd ed. (1974).
[18] G.J. Hutchings, C.J. Kiely, M.T. Sananes-Schulz, A. Burrows and J.C. Volta, Catal. Today 58 (1998) 273.
[19] Y.H. Taufiq-Yap, M.H. Looi, K.C. Waugh, M.Z. Hussein, Z. Zainal and R. Samsuddin, Catal. Lett. 74 (2001) 99.
[20] K.C. Waugh and Y.H. Taufiq-Yap, Catal. Today 81 (2003) 215.
[21] K.P. Tan, *PhD Thesis*, Universiti Putra Malaysia (2004).
[22] T. Ushikubo, H. Nakamura, Y. Koyasu, S. Wajiki, US Patent 5,380,933 (1995).
[23] M. Takahashi, S. To, S. Hirose, JP Patent, 98,120,617 (1998).
[24] D. Vitry, J.L. Dubois and W. Ueda, J. Mol. Catal. A:Chem. 220 (2004) 67.
[25] H. Chong, Y. Han and H. Wang, Shiyou Huagong (Chinese) 28 (1999) 803.